Chapter 28
Ground motion selection for performance-based engineering: Effect of target spectrum and conditioning period

Jack W. Baker, Ting Lin and Curt B. Haselton

Abstract This chapter presents a study of the impact of conditioning period on structural analysis results obtained from ground motions selected using the Conditional Spectrum concept. The Conditional Spectrum provides a quantitative means to model the distribution of response spectra associated with ground motions having a target spectral acceleration at a single conditioning period. One previously unresolved issue with this approach is how to condition this target spectrum for cases where the structure of interest is sensitive to excitation at multiple periods due to nonlinearity and multi-mode effects. To investigate the impact of conditioning period, we perform seismic hazard analysis, ground motion selection, and nonlinear dynamic structural analysis to develop a "risk-based" assessment of a 20-story concrete frame building. We perform this assessment using varying conditioning periods and find that the resulting structural reliabilities are comparable regardless of the conditioning period used for seismic hazard analysis and ground motion selection. This is true as long as a Conditional Spectrum (which carefully captures trends in means and variability of spectra) is used as the ground motion target, and as long as the analysis goal is a risk-based assessment that provides the annual rate of exceeding some structural limit state (as opposed to computing response conditioned on a specified ground motion intensity level). Theoretical arguments are provided to support these findings, and implications for performance-based earthquake engineering are discussed.

Keywords: Ground motion selection, seismic risk assessment, nonlinear analysis

28.1 Introduction

Recent work has illustrated that scaling up arbitrarily selected ground motions to a specified spectral acceleration (*Sa*) level at period *T* can produce overly conservative structural responses, because a single extreme *Sa*(*T*) level of interest for engineering analysis does not imply occurrence of equally extreme *Sa* levels at all periods. The

J. Baker
Stanford University, Department of Civil & Environmental Eng., 473 Via Ortega MC 4020, Stanford, USA
e-mail: bakerjw@stanford.edu

Conditional Mean Spectrum (CMS) and Conditional Spectrum (CS) have been developed to describe the expected response spectrum associated with a ground motion having a specified *Sa(T)* level (Baker and Cornell 2006; Baker 2011; Lin et al. 2012). The Conditional Mean Spectrum for a rare (i.e., positive ε) $Sa(T)$ level has a relative peak at T and tapers back towards the median spectrum at other periods. The Conditional Spectrum differs from the Conditional Mean Spectrum in that it also considers the variability in response spectra at periods other than the conditioning period (which by definition has no variability).

The Conditional Spectrum approach for selecting and scaling ground motions requires the user to specify a conditioning period (denoted here as T^*) that is used to compute corresponding distributions of spectral values at all other periods. Ground motions can then be selected to match these spectral values, and used as inputs to dynamic structural analysis, to compute Engineering Demand Parameters, or *EDP*s. When calculating Peak Story Drift Ratio (*PSDR*) in buildings, T^* is often chosen to be the building's elastic first-mode period (T_1). This is done because $Sa(T_1)$ is often a "good" predictor of that *EDP*, so scaling ground motions based on this parameter can lead to reduced scatter in resulting response predictions and thus minimizes the required number of dynamic analyses (Shome et al. 1998).

There are situations where the application of the CS concept is not yet straightforward. One such situation is for prediction of *EDP*s which are not dominated by the first-mode structural response, due to contributions from higher modes, such as peak floor accelerations, or to longer periods associated with reduced-stiffness nonlinear response such as the onset of collapse (Haselton and Baker 2006). A second situation is for selection of ground motions prior to identification of a single conditioning period, because the structure is not yet designed or because multiple designs having multiple periods are being considered. In both cases, one is faced with the possibility of using a Conditional Spectrum that is not conditioned on *Sa* at the period that most efficiently predicts structural response. And even in cases where one does know an effective conditioning period for computing the CS, the question still arises as to whether a comparable-intensity *Sa* at some other conditioning period might produce a larger level of *EDP*s than the primary CS being considered.

Here we will demonstrate that, *if* the analysis objective is to compute the annual rate of the structure experiencing $EDP > y$, and *if* the ground motions are selected to match the Conditional Spectrum, then the resulting answer is relatively insensitive to the choice of conditioning period. While some researchers have previously suggested that the choice of conditioning period may not be critical to estimates of reliability (e.g., Abrahamson and Yunatci 2010; Shome and Luco 2010), those efforts did not perform a full risk-based assessment using nonlinear dynamic analyses, and did not consider spectral variability at periods other than the conditioning period. Here we do repeated risk-based assessments (i.e., compute the rate of $EDP > y$ using nonlinear dynamic

analysis at multiple *Sa* levels) to demonstrate this statement empirically. We also present theoretical arguments and intermediate results to support these findings.

28.2 Demonstration Analysis

To illustrate the effect of conditioning period, we first perform two parallel performance assessments, using ground motions selected to match Conditional Spectra conditioned on two periods. We will later look at the effect of repeating the procedure using other conditioning periods. The test case and analysis procedure is described in this section.

28.2.1 Building site and structural model

The structure being studied is assumed to be located in Palo Alto, California, approximately 10 km from the San Andreas Fault. The structure is a 20-story reinforced concrete special moment frame with the perimeter frame designed to resist lateral forces. This building was designed for the recent FEMA P695 project (Federal Emergency Management Agency 2009; Haselton and Deierlein 2007), and is denoted Building 1020 in that study. It is modeled in OpenSEES (2011), with strength deterioration (both cyclic and in-cycle) and stiffness deterioration that is believed to reasonably capture the responses up to the point of dynamic-instability collapse. The first three elastic modal periods are 2.6s, 0.85s and 0.45s. The building was designed per the ICC (2003), for a site with a slightly lower design ground motion level than the site being utilized in this study (by approximately 20%). Estimating the annual rate of exceeding various thresholds of Peak Story Drift Ratio in this building is not trivial, as the *PSDR* is affected by multiple modes excited at multiple periods, and experiences effective period lengthening as it behaves nonlinearly up to the collapse level for high intensity ground motions.

28.2.2 Seismic hazard analysis and ground motion selection

We perform seismic hazard analysis to obtain ground motion hazard curves for spectral accelerations at three periods (0.85s, 2.6s and 5s), corresponding to the first two modal periods of the building and a lengthened period that may be a good predictor of nonlinear response. For each spectral period and amplitude of interest, we obtain the rate of exceeding that amplitude and a deaggregation distribution providing the causal magnitudes, distances and ε values associated with spectral accelerations of that amplitude. All of this data comes from the U.S. Geological Survey online tools (USGS 2008). Ten rates of exceedance are considered for each conditioning period, ranging from 0.023 to 0.00005 per year (i.e., 50% in 30 years to 1% in 200 years probability of exceedance), as those are the exceedance rates for which the USGS provides the needed

hazard and deaggregation information. Hazard curves and deaggregation results are not provided for exactly the conditioning periods used here, so interpolation between hazard results at adjacent periods is utilized.

Using the hazard curve and deaggregation information for a particular conditioning period, the Conditional Spectrum calculation is used to compute the mean and standard deviation of logarithmic response spectral values at all other periods, conditioned on an amplitude of $Sa(T^*)$. The mean and standard deviation of lnSa are given by the following equations (Baker and Cornell 2005a; Baker 2011)

$$\mu_{\ln Sa(T_i)|\ln Sa(T^*)} = \mu_{\ln Sa}(M,R,T_i) + \rho(T_i,T^*)\varepsilon(T^*)\sigma_{\ln Sa}(T_i) \quad (1)$$

$$\sigma_{Sa(T_i)|Sa(T^*)} = \sigma_{\ln Sa}(T_i)\sqrt{1-\rho^2(T_i,T^*)} \quad (2)$$

where $\mu_{\ln Sa}(M,R,T_i)$ and $\sigma_{\ln Sa}(T_i)$ are the predicted mean and standard deviation from a ground motion prediction model (Boore and Atkinson 2008 in this case), $\rho(T_i,T^*)$ is the correlation between the spectral values at period T and the conditioning period T^* (obtained from Baker and Jayaram 2008), and M, R and $\varepsilon(T^*)$ come from the deaggregation distributions described in the previous section. In this case the M, R and $\varepsilon(T^*)$ values used are the mean values from deaggregation at the given $Sa(T^*)$ level; this is an approximation relative to the use of the full distributions of potential M, R and $\varepsilon(T^*)$ values, and performing a more exact calculation is possible and important to do in some cases as discussed in detail by Lin (2012).

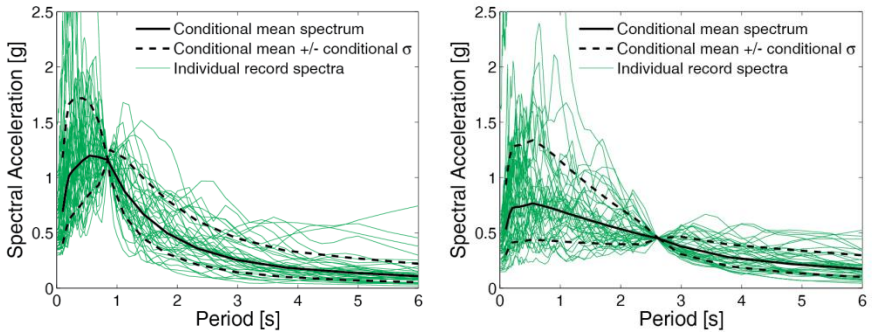

(a) (b)

Figure 28-1: Conditional spectra and spectra of selected ground motions for a site at Palo Alto, California, with spectral acceleration at the conditioning period having a 2% probability of exceedance in 50 years, (a) conditioned on $Sa(0.85s) = 1.2g$, (b) conditioned on $Sa(2.6s) = 0.45g$.

For each conditioning period and spectral amplitude, forty recorded ground motions were selected and scaled such that their spectra matched the target mean and standard

deviations computed using equations 1 and 2. Figure 28-1 shows the target spectra and selected ground motions' spectra for 0.85s and 2.6s conditioning periods, at *Sa* amplitudes with 2% probability of exceedance in 50 years. Ground motions were selected from the PEER NGA database (Chiou et al. 2008). No further constraints were placed on the ground motion selection (e.g., magnitudes and distances) other than limiting scale factors to less than four, with the primary selection focus being on the match of the ground motion spectra to the target spectra. This was done because the structure response parameter of interest in this case is thought to be most closely related to spectral values, and that earthquake magnitude and distance affect this structural response primarily as they relate to spectral values (which are accounted for directly through the Conditional Spectrum) rather than other ground motion parameters such as duration. Details regarding the ground motion selection algorithm and its implications are provided by Jayaram et al. (2011).

28.2.3 Structural analysis and risk assessment

With the selected ground motions (40 motions at each of 10 intensity levels, for a given conditioning period), dynamic analysis of the structure described above was performed. Results are shown in Figure 28-2 for the ground motions selected conditioned on two periods, and the fraction of ground motions causing collapse at each conditioning period and *Sa* level are shown in Figure 28-3 (in this figure, results from ground motions with a third conditioning period of 5s are also shown). A collapse fragility curve was obtained using a maximum likelihood approach to fit a lognormal fragility function to those observed fractions of collapse (Baker and Cornell 2005b, Appendix D).

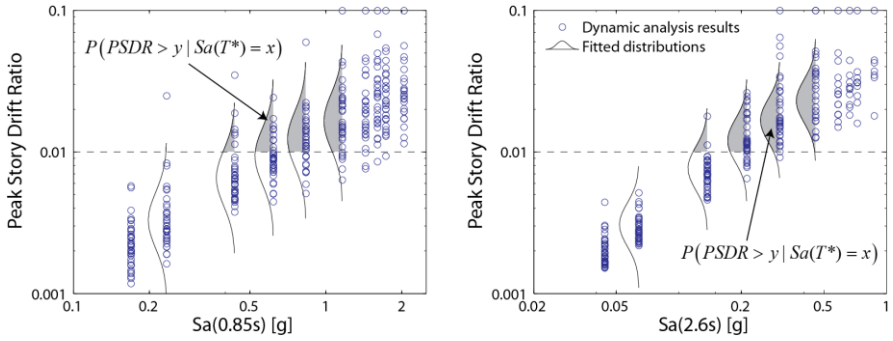

(a) (b)

Figure 28-2: Peak Story Drift Ratios from non-collapse dynamic structural analysis, and fitted probability distributions, for ground motions selected to match Conditional Spectra with (a) T^* = 0.85s and (b) T^* = 2.6s.

For our risk-based assessment the structural analysis results are combined with the hazard curve for the corresponding conditioning *Sa*, to compute the annual rate of exceeding a given *PSDR* level as follows:

$$\lambda\left(PSDR > y\right) = \int_{x} P\left(PSDR > y \mid Sa(T^*) = x\right) \left| d\lambda\left(Sa(T^*) > x\right) \right| \qquad (3)$$

where $d\lambda\left(Sa(T^*) > x\right)$ is the derivative of the hazard curve for $Sa(T^*)$, $P\left(PSDR > y \mid Sa(T^*) = x\right)$ is the probability of Peak Story Drift Ratio exceeding y given a ground motion with $Sa(T^*) = x$, and $\lambda\left(PSDR > y\right)$ is the rate of Peak Story Drift Ratio exceeding y. The $P\left(PSDR > y \mid Sa(T^*) = x\right)$ term is computed as follows

$$P\left(PSDR > y \mid Sa(T^*) = x\right) = P(C) + \left(1 - P(C)\right)\left(1 - \Phi\left(\frac{\ln y - \mu_{\ln PSDR}}{\beta_{\ln PSDR}}\right)\right) \qquad (4)$$

where $P(C)$ is the probability of collapse given $Sa(T^*) = x$ estimated from the collapse fragility function in Figure 28-3, $\mu_{\ln PSDR}$ and $\beta_{\ln PSDR}$ are the mean and standard deviation, respectively, of ln*PSDR* values given $Sa(T^*) = x$ in Figure 28-2, and $\Phi()$ is the standard normal distribution cumulative distribution function. This approach assumes that all collapse cases exceed *y*, and fits a lognormal distribution to the non-collapse *PSDR*s, following procedures proposed elsewhere (e.g., Shome and Cornell 1999).

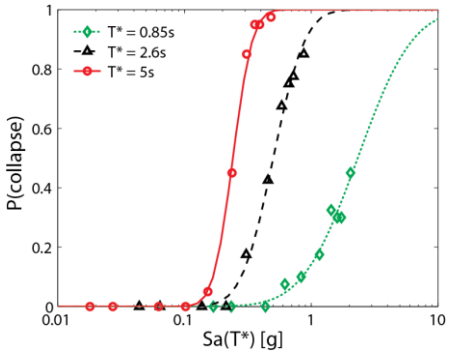

Figure 28-3: Observed fractions of analyses causing collapse from ground motions selected to match Conditional Spectra with three conditioning periods, and fitted fragility functions.

The calculation in equation 3 is referred to here as a risk-based assessment, though it is also referred to elsewhere as the first step of the "PEER Integral," (Cornell and Krawinkler 2000), a "drift hazard" calculation (Krawinkler and Miranda 2004), or a "time-based assessment" (Applied Technology Council 2011). Equation 3 was

evaluated using the three sets of hazard curves, ground motions and resulting structural responses associated with each of the considered T^* values, and the resulting risk assessment results are shown in Figure 28-4. The predictions of the rates of exceeding a given *PSDR* are very consistent regardless of the conditioning period.

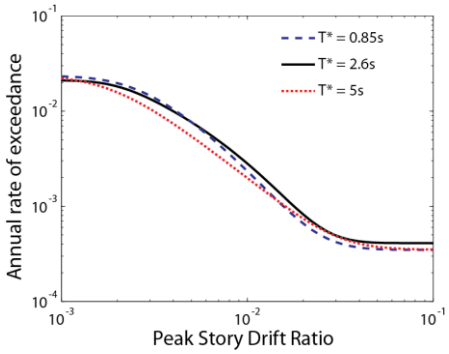

Figure 28-4: Risk assessment results showing annual rates of exceedance for various Peak Story Drift Ratios, obtained using hazard curves and ground motions with three different conditioning periods.

The relative consistency of results in Figure 28-4 may be surprising at first, so let us examine the data underlying these results more closely. In Figure 28-5a and Figure 28-5b, we see the response spectra of the ground motions selected and scaled to match *Sa*(2.6s) and *Sa*(0.85s) at the ten amplitudes considered; we see the "pinched" shapes of the spectra at 0.85s and 2.6s in Figure 28-5a and Figure 28-5b, respectively, at those ten conditioning amplitudes. At other periods, the spectra are more varied, as the amplitudes at other periods have variability even when *Sa*(T^*) is known with certainty. But the careful way in which these ground motions were selected, to maintain proper conditional means and variances, ensures that the distributions of spectra at all periods are still consistent with all known hazard information for the site being considered. It is difficult to see this consistency visually in Figure 28-5a and b, because there are 40 ground motions at each *Sa* amplitude, while the real site will have many more low-amplitude ground motions than high-amplitude motions (and equation 3 captures this by incorporating weights from the hazard curve).

To make a quantitative comparison of the sets of response spectra, the rate of *Sa* exceeding a given amplitude *y* at an arbitrary period *T*, implied by the ground motions selected conditional on *Sa*(T^*), is computing using an equation very similar to equation 3

$$\lambda\left(Sa(T)>y\right)=\int_{x} P\left(Sa(T)>y \mid Sa(T^*)=x\right)\left|d\lambda\left(Sa(T^*)>x\right)\right| \qquad (5)$$

where $P\left(Sa(T) > y \mid Sa(T^*) = x\right)$ is the probability that a ground motion in the selected record set to have $Sa(T^*) = x$ has an Sa at period T that is greater than y. Here this probability is estimated as simply the fraction of the 40 ground motions with $Sa(T^*) = x$ that have $Sa(T) > y$. The multiplication of these probabilities by the derivative of the hazard curve reweights the results according to the rate of observing ground motions with $Sa(T^*) = x$, as was done in equation 3.

Figure 28-5c shows the implied rate of $Sa(2.6s) > y$ for the ground motions in Figure 28-5a and b, plus comparable ground motions with $T^* = 5s$. Additionally, the hazard curve for $Sa(2.6s)$ is plotted, as this is the correct answer from hazard analysis that we are trying to represent using a suite of ground motions. The ground motions selected using $T^* = 2.6s$ have a stepped plot in Figure 28-5c, due to the ten discrete $Sa(2.6s)$ amplitudes that were considered when selecting motions. The ground motions with other T^* values have smoother curves, but all of the curves are in good general agreement, indicating that even though the other sets of ground motions did not scale ground motions to match $Sa(2.6s)$, they have the proper distribution of $Sa(2.6s)$ as specified by the hazard curve at that period. Thus, if $Sa(2.6s)$ is a good predictor of structural response, then the ground motions selected to match $Sa(0.85s)$ will still do a good job of capturing the distribution of structural response values that might be observed for the given site and structure considered. A similar plot is shown in Figure 28-5d for the rate of exceeding $Sa(5s)$; in this case the ground motions with $T^* = 5s$ have the stepped curve, and the other T^* cases are smooth. Again the curves are in relatively good agreement with each other, and with the true ground motion hazard curve.

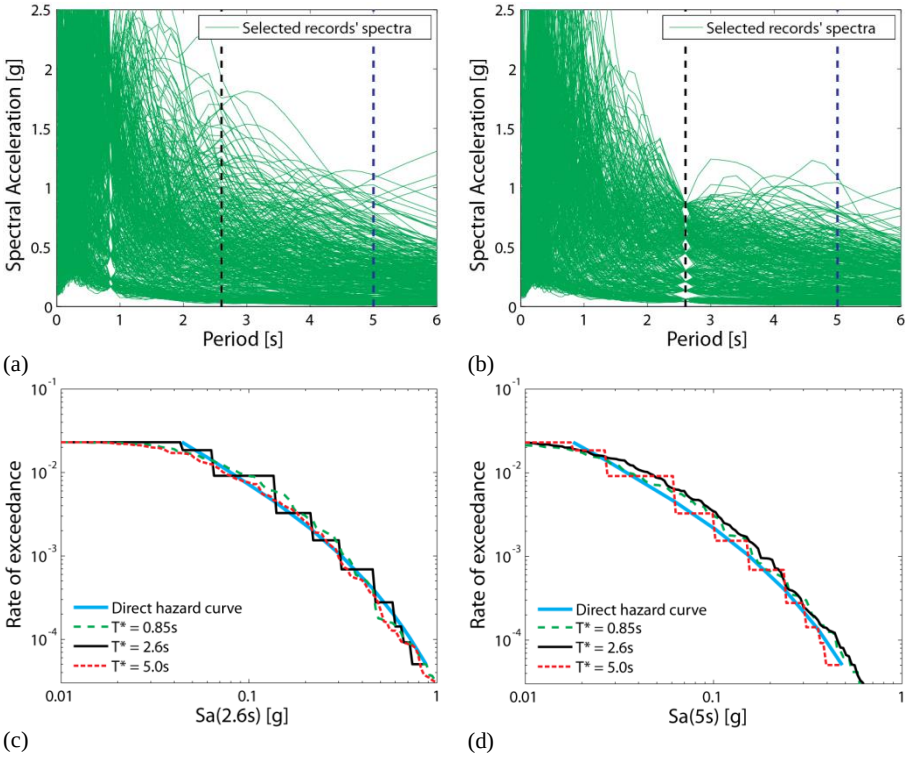

Figure 28-5: (a) Response spectra of ground motions selected using T^* = 0.85s. (b) Response spectra of ground motions selected using T^* = 2.6s. (c) Rate of Sa(2.6s) > y implied by each of the selected ground motion sets, plus the original ground motion hazard curve for reference. (d) Rate of Sa(5s) > y implied by each of the selected ground motion sets, plus the original ground motion hazard curve for reference.

28.3 Discussion

In principle, equation 3 is correct regardless of the value used to quantify intensity, but a few assumptions inherent in the application of this equation place practical constraints on this evaluation. First, equation 3 assumes that $P\left(PSDR > y \mid Sa(T^*) = x\right)$ is not dependent upon other ground motion properties besides the one quantified by the intensity measure, although this is never true for structures other than elastic single-degree-of-freedom systems (Luco and Cornell 2007). Here we have addressed that problem by further accounting for the effect of spectral values at other periods through ground motion selection with Conditional Spectrum targets, such that spectral values at all periods in the selected ground motions are consistent with hazard curves for the site,

regardless of the spectral period used for conditioning. Nonetheless, we have only considered spectral values and not other ground motion properties (e.g. velocity pulses not fully captured in the spectral acceleration values, duration, etc.). If non-spectral ground motion parameters were also deemed important for predicting the *EDP* of interest, the approach above can be generalized to account for those parameters (Bradley 2010).

Another limitation of the approach used here is that equations 1 and 2 used for computing the target Conditional Spectra are approximate if only a single magnitude and distance value is input, or only a single ground motion prediction model is used, because the calculations that produced the hazard curves use multiple magnitudes, distances and ground motion prediction models. That approximation was reasonable for the cases considered here, but is known to be unreasonable for many other cases. More exact uses of equations 1 and 2 are available in (Lin et al. 2012), and the impact of this refinement is the subject of more detailed discussion in (Lin 2012).

28.4 Conclusions

We have presented risk-based assessment results for Peak Story Drift Ratios in a 20-story concrete frame structure located in Palo Alto, California, using a structural model with strength and stiffness deterioration that is believed to reasonably capture the responses up to the point of dynamic-instability collapse. The assessment was performed three times, using ground motions selected and scaled to match Conditional Spectra at three conditioning periods from 0.85s to 5.0s (i.e., the second-mode structural period up to twice the first-mode period). For each case, the risk-based assessment results were similar. This similarity stems from the fact that the careful record selection ensures that the distributions of response spectra at all periods are consistent with targets specified by hazard analysis, so the distribution of resulting story drifts should also be comparable (to the extent that response spectra describe the relationship between the ground motions and structural responses).

From these results, we observe if the analysis goal is to perform a full "risk assessment" calculation, then one should be able to obtain an accurate result using any conditioning period, as long as careful ground motion selection ensures proper representation of spectral values and other ground motion parameters of interest. Here "proper representation" refers to consistency with the site ground motion hazard curves at all relevant periods, and this is achieved by using the Conditional Spectrum approach to determine target response spectra for the selected ground motions. The reproducibility of the results with varying conditional periods then results from the fact that the ground motion intensity measure used to link the ground motion hazard and the structural response is not an inherent physical part of the seismic reliability problem we are considering; it is only a useful link to decouple the hazard and structural analysis. If

this link is maintained carefully then one should get a consistent answer (the correct answer) for the risk assessment in every case. The consistency in risk assessments achieved here is in contrast to some previous speculation on this topic, because this study utilizes the recently developed Conditional Spectrum target for ground motion selection, and uses a newly available algorithm for selecting ground motions to match this target.

Is the choice of conditioning period still important? Choice of a "good" conditioning period does still serve several useful purposes. A good conditioning period helps because the spectral accelerations at the conditioning period will be a good predictor of structural response; this makes any inaccuracies in representing spectral values at other periods have a less severe impact on the resulting calculations. Additionally, use of a good conditioning period reduces the variability in structural responses and thus reduces the number of dynamic analyses that are required to accurately estimate distributions of structural response. Luco and Cornell (2007) referred to these two properties as "sufficiency" and "efficiency," respectively. We take those concepts further here, acknowledge that there is no intensity measure with perfect efficiency and sufficiency, and so perform careful ground motion selection to compensate for shortcomings that are inherent in any intensity measure.

This document has presented a relatively simple illustration of the concept that hazard consistency in ground motions will lead to consistent risk-based assessment results. This work is part of a larger project on ground motion selection (NIST 2011), and the PhD thesis of Ting Lin (2012) provides a much more extensive set of analyses of this type, including studies of permutations on the target spectrum used, the *EDP* parameter of interest, and the type of structure being analyzed. Those results provide a more complete picture of the relationship between careful ground motion selection and robust structural response results.

28.5 Acknowledgements

This work was supported in part by the NEHRP Consultants Joint Venture (a partnership of the Consortium of Universities for Research in Earthquake Engineering and Applied Technology Council), under Contract SB134107CQ0019, Earthquake Structural and Engineering Research, issued by the National Institute of Standards and Technology, for project ATC-82. Any opinions, findings and conclusions or recommendations expressed in this material are those of the authors and do not necessarily reflect those of the NEHRP Consultants Joint Venture. The authors also acknowledge the contributions of Jared DeBock and Fortunato Enriquez in conducting the structural analyses used in this study.

References

Abrahamson, N. A., and Yunatci, A. A. (2010). "Ground Motion Occurrence Rates for Scenario Spectra." *Fifth International Conference on Recent Advances in Geotechnical Earthquake Engineering and Soil Dynamics*, San Diego, California, Paper No. 3.18, 6p.

Applied Technology Council. (2011). *ATC-58, Guidelines for Seismic Performance Assessment of Buildings, 75% Draft*. Applied Technology Council, Redwood City, California, 266p.

Baker, J. W. (2011). "Conditional Mean Spectrum: Tool for ground motion selection." *Journal of Structural Engineering*, 137(3), 322–331.

Baker, J. W., and Cornell, C. A. (2005a). "A vector-valued ground motion intensity measure consisting of spectral acceleration and epsilon." *Earthquake Engineering & Structural Dynamics*, 34(10), 1193–1217.

Baker, J. W., and Cornell, C. A. (2005b). *Vector-valued ground motion intensity measures for probabilistic seismic demand analysis*. Report No. 150, John A. Blume Earthquake Engineering Center, Stanford, CA, 321p.

Baker, J. W., and Cornell, C. A. (2006). "Spectral shape, epsilon and record selection." *Earthquake Engineering & Structural Dynamics*, 35(9), 1077–1095.

Baker, J. W., and Jayaram, N. (2008). "Correlation of spectral acceleration values from NGA ground motion models." *Earthquake Spectra*, 24(1), 299–317.

Boore, D. M., and Atkinson, G. M. (2008). "Ground-Motion Prediction Equations for the Average Horizontal Component of PGA, PGV, and 5%-Damped PSA at Spectral Periods between 0.01 s and 10.0 s." *Earthquake Spectra*, 24(1), 99–138.

Bradley, B. A. (2010). "A generalized conditional intensity measure approach and holistic ground-motion selection." *Earthquake Engineering & Structural Dynamics*, 39(12), 1321–1342.

Chiou, B., Darragh, R., Gregor, N., and Silva, W. (2008). "NGA Project Strong-Motion Database." *Earthquake Spectra*, 24(1), 23–44.

Cornell, C. A., and Krawinkler, H. (2000). "Progress and Challenges in Seismic Performance Assessment." *PEER Center News*, 3(2).

Federal Emergency Management Agency. (2009). *Quantification of Building Seismic Performance Factors (FEMA P695, ATC-63)*. FEMA P695, prepared by the Applied Technology Council, 421p.

Haselton, C. B., and Deierlein, G. G. (2007). *Assessing seismic collapse safety of modern reinforced concrete moment frame buildings*. Pacific Earthquake Engineering Research Center, Berkeley, CA.

Haselton, C., and Baker, J. W. (2006). "Ground motion intensity measures for collapse capacity prediction: choice of optimal spectral period and effect of spectral shape." *Proceedings, 8th National Conference on Earthquake Engineering*, San Francisco, California, 10.

ICC. (2003). *International Building Code 2003*. International Code Council, ICC (distributed by Cengage Learning).

Jayaram, N., Lin, T., and Baker, J. W. (2011). "A computationally efficient ground-motion selection algorithm for matching a target response spectrum mean and variance." *Earthquake Spectra*, 27(3), 797–815.

Krawinkler, H., and Miranda, E. (2004). "Performance-based earthquake engineering." *Earthquake Engineering: From Engineering Seismology to Performance-Based Engineering (edited by Y. Bozorgnia and VV Bertero)", CRC Press, Boca Raton, USA*.

Lin, T. (2012). *Advancement of hazard consistent ground motion selection methodology*. PhD Thesis, Dept. of Civil and Environmental Engineering, Stanford University, Stanford, CA.

Lin, T., Harmsen, S. C., Baker, J. W., and Luco, N. (2012). "Conditional Spectrum Computation Incorporating Multiple Causal Earthquakes and Ground Motion Prediction Models." *Bulletin of the Seismological Society of America*.

Luco, N., and Cornell, C. A. (2007). "Structure-Specific Scalar Intensity Measures for Near-Source and Ordinary Earthquake Ground Motions." *Earthquake Spectra*, 23(2), 357–392.

NIST. (2011). *Selecting and Scaling Earthquake Ground Motions for Performing Response-History Analyses*. NIST GCR 11-917-15, Prepared by the NEHRP Consultants Joint Venture for the National Institute of Standards and Technology, Gaithersburg, Maryland.

OpenSEES. (2011). "Open system for earthquake engineering simulation." *Pacific Earthquake Engineering Research Center*, <http://opensees.berkeley.edu/> (Jun. 20, 2011).

Shome, N., and Cornell, C. A. (1999). *Probabilistic seismic demand analysis of nonlinear structures*. Report No. RMS35 (Ph.D. Thesis), RMS Program, Stanford, CA, 320.

Shome, N., Cornell, C. A., Bazzurro, P., and Carballo, J. E. (1998). "Earthquakes, Records, and Nonlinear Responses." *Earthquake Spectra*, 14(3), 469–500.

Shome, N., and Luco, N. (2010). "Loss estimation of multi-mode dominated structures for a scenario of earthquake event." *9th US National and 10th Canadian Conference on Earthquake Engineering*, Toronto, Canada, 10.

USGS. (2008). "Interactive Deaggregation Tools." *United States Geological Survey*, <https://geohazards.usgs.gov/deaggint/2008/> (Jun. 20, 2011).

Keywords:
Nonlinear dynamic analysis, ground motions, ground motion selection, ground motion scaling, Uniform Hazard Spectrum, UHS, Conditional Mean Spectrum, CMS, Conditional Spectrum, structural reliability, seismic risk, probabilistic seismic hazard analysis, PSHA, deaggregation, response spectrum, probability distribution, spectral acceleration, hazard consistency, conditioning period